STRUCTURAL
CHEMISTRY

Volume 74 (2018)

Supporting information for article:

Novel tantalum phosphate Na13Sr2Ta2(PO4)9: synthesis, crystal structure, DFT calculations and Dy^{3+}-activated fluorescence performance

Ji Zhao, Dan Zhao, Ya-Li Xue, Qiu Zong, Shi-Rui Zhang and Bao-Zhong Liu

1.

2. Experiment section

2.1. Materials and instrumentations

NaH_2PO_4 (AR, ≥99.0%), $SrCO_3$ (AR, ≥99.0%), Ta_2O_5 (AR, ≥99.99%) and Na_2CO_3 (AR, ≥99.8%) were used as received from Sinopharm Chemical Reagent Co., Ltd. The X-ray powder diffraction (XRD) analysis were performed by Rigaku SmartLab 9KW dffractormeter with graphite-monochromated CuKα characteristic radiation, operating at 200 mA, 40 kV; scanning speed, step length and diffraction range were 10°/min^{-1}, 0.02° and 5–75°. The sizes and morphologies of the phosphors were inspected using a scanning electron microscope (Carl Zeiss AG, Merlin Compact). UV-Vis diffuse reflectance spectroscopy (DRS) properties were studied on a Lambda 950 UV/Vis Spectrophotometer (PerkinElmer company) equipped with an integrating $BaSO_4$ sphere in the wavelength range of 200~800 nm at room temperature. Photoluminescence (PL) spectra were carried out by a FLuorolog-3 combined time Resolved & steady state fluorescence spectrometer (HORIBA Company). The step width is 1 nm and integration time is 0.2 s.

2.2. Synthetic procedures

$Na_{13}Sr_2Ta_2(PO_4)_9$ was prepared in single-crystal form by dissolving $SrCO_3$ and Ta_2O_5 in a sodium phosphate melt as follows: a mixture of 3.000 g of NaH_2PO_4 (25.00 mmol), 0.3690 g of $SrCO_3$ (2.500 mmol), 0.3683 g of Ta_2O_5 (0.8333 mmol) and 0.4417 g of Na_2CO_3 (4.167 mmol), was thoroughly ground in an agate mortar and pre-fused at 950 °C in a platinum crucible. The final weight of the transparent melt roughly corresponded with that expected from the loss of the appropriate amounts of H_2O and CO_2. Heating the crucible at 950 °C for 4 h, followed by a slow cool to 650 °C at the rate of 4 °C/h gave clear syrup over a few small crystals of $Na_{13}Sr_2Ta_2(PO_4)_9$ and some unknown white powders. These colourless parallelepiped crystals can be selected for structural analysis by washing adhering flux with water. A series of powder samples $Na_{13}Sr_{2-x}Ta_2(PO_4)_9$:$x$Dy^{3+} ($x$=0, 0.01, 0.02, 0.04, 0.06, 0.08, 0.10, 0.12, 0.14) were prepared by grinding a stoichiometric ratio of NaH_2PO_4, $SrCO_3$, Ta_2O_5, Na_2CO_3 and Dy_2O_3 under ethanol and then heating the mixture in an platinum crucible at 780 °C for 48 hours; the heating was interrupted several times for additional grinding of the samples. Powder X-ray diffraction (XRD) has been studied at room temperature, which can be comparable with the pattern simulated from the single-crystal data using Jana2006 software (Petricek *et al.*, 2014). As shown in Fig. 1 and Fig. S1 (see ESI), no additional peaks were observed, implying the pure powders $Na_{13}Sr_{2-x}Ta_2(PO_4)_9$:$x$Dy^{3+} were successfully obtained without any impurity phases. Considering the similar ionic radius of Dy^{3+} and Sr^{2+} ions, we confirm that Dy^{3+} can replace the sites of Sr^{2+} to form a solid solution of $Na_{13}Sr_{2-x}Ta_2(PO_4)_9$:$x$Dy^{3+} without changing the crystal structure.

2.3. Crystallography

A suitable crystal with dimensions 0.20 × 0.20 × 0.04 mm for $Na_{13}Sr_2Ta_2(PO_4)_9$ was selected for data collection on a Bruker Smart Apex2 CCD area detector with a graphite-monochromated Mo/Kα radiation of λ = 0.71073 Å, and a tube power of 50 kV × 20 mA. The lattice constants were determined by a least-squares analysis of 617 reflections that had been cantered on detector in the range of 2.38º < 2θ < 24.50º. The data were collected with the ω-2θ scan technique. The reflections were corrected far Lorentz, polarization and secondary extinction effects. Multi-scan absorption correction was performed using the SADABS software involved in Apex2 package (Bruker, 2014). The crystal structure was solved and refined with the program Shelx-2014 from Apex2 crystallographic software package (Sheldrick, 2015). The positions of the atoms Sr, Ta, and P were determined from direct method, and the Na and O atoms were located from subsequent analyses of difference electron density maps. Interestingly, our prepared crystal of $Na_{13}Sr_2Ta_2(PO_4)_9$ is twinning, although the appearance looks very fine. If this twinning is ignored, the refinement would be hardly continued. A merohedral twin law (-1 0 0 1 1 0 0 0 -1) can be derived from the relation between the real point group '6/m' and apparent point group '6/mmm', which can be introduced in the refinement. Meanwhile, a 'Basf 0.5' instruction was added in the *.ins file to refine the twin ratio, suggesting a value of 0.603 : 0.397. Final least-squares refinement on F^2 with anisotropic thermal parameters on each atom resulted in the final residuals R = 1.9 %, wR = 4.2 %. And the final difference Fourier maps showed featureless highest residual peak of 0.60 at 1.11 Å from O(4) atom, and the deepest hole is -1.32 at 0.74 Å from Ta(1) which may be caused by strong absorption for heavy atoms. Results imply that such a twinning structure model for $Na_{13}Sr_2Ta_2(PO_4)_9$ is reasonable. If this twinning is ignored, or removes the Twin and Basf instructions in the *.ins file, the final refinement will lead to unaccepted residuals of R = 13.1 %, wR = 47.8 %, and the residual peaks and holes will be up to 12.77 and -5.11. Therefore, we confirmed that the twin. The CIF was checked using software PLATON package (Spek, 2009), showing no A and B errors. Tab. 1 presents the details of data structure solution and refinement. Selected bond lengths and angles are tabulated in Tab. 2. Atomic positional parameters and isotropic temperature factors are presented in Tab. S1 and S2, given as supporting information. Further details of the crystal structure can be obtained from the ICSD database (Fachinformationszentrum Karlsruhe), on quoting the depository numbers of CSD-434285 for $Na_{13}Sr_2Ta_2(PO_4)_9$.

2.4. Computational descriptions

The single crystal data of $Na_{13}Sr_2Ta_2(PO_4)_9$ were used to make an total-energy calculation by CASTEP code (Segall *et al.*, 2002) without geometry optimization. The pseudo-potentials were employed to describe electron-ion interactions and electronic wave functions with a plane-wave basis. The total energy and properties were calculated within the framework of the Perdew-Burke-Ernzerhof generalized gradient approximation (GGA-PBE) (Perdew *et al.*, 1996). In addition, the norm-conserving pseudo-potentials (M. C. Payne, 1992) were employed for Na, Sr, Ta, P and O atoms,

respectively. The total energy and the force convergence thresholds were 1.0×10^{-6} eV/atom and 0.05 eV/Å, respectively. The *k*-point set meshes to define the number of integration points that will be used to integrate the wave function in reciprocal space were 3 × 3 × 2 for calculating bond structure and density of state (Monkhorst, 1977). The rest parameters used in the calculations were set by the default values of the CASTEP code. Pseudo atom calculations were performed for Na-2$s^2$2$p^6$3s^1, Sr-4$s^2$4$p^6$5s^2, Ta-5$d^3$6s^2, P-3$s^2$3p^3 and O-2$s^2$2p^4.

Table S1 Fractional atomic coordinates and isotropic displacement parameters (Å^2) of $Na_{13}Sr_2Ta_2(PO_4)_9$

$Na_{13}Sr_2Ta_2(PO_4)_9$	*x*	*y*	*z*	U_{iso}*/U_{eq}
Na1	0.03444 (18)	0.35671 (19)	0.04715 (6)	0.0214 (3)
Na2	0.333333	0.666667	0.17305 (11)	0.0218 (6)
Na3	0.3865 (3)	0.3975 (3)	0.250000	0.0150 (4)
Na4	0.666667	0.333333	0.00910 (9)	0.0141 (5)
Sr1	0.666667	0.333333	0.16076 (2)	0.00917 (11)
Ta1	0.000000	0.000000	0.14844 (2)	0.00495 (8)
P1	0.34762 (11)	0.33999 (11)	0.09335 (3)	0.00755 (16)
P2	0.28920 (15)	0.01818 (16)	0.250000	0.0055 (2)
O1	0.4195 (4)	0.4350 (4)	0.14930 (10)	0.0196 (6)
O2	0.4403 (3)	0.2445 (3)	0.07626 (10)	0.0166 (6)
O3	0.3452 (4)	0.4536 (3)	0.04555 (11)	0.0192 (6)
O4	0.1498 (3)	0.1977 (3)	0.10115 (9)	0.0112 (6)
O5	0.1934 (3)	0.0383 (3)	0.19715 (11)	0.0182 (6)
O6	0.2812 (4)	−0.1514 (4)	0.250000	0.0135 (8)
O7	0.4687 (4)	0.1709 (4)	0.250000	0.0082 (7)

Table S2 Atomic anisotropic displacement parameters (Å^2) of $Na_{13}Sr_2Ta_2(PO_4)_9$.

$Na_{13}Sr_2Ta_2(PO_4)_9$	U^{11}	U^{22}	U^{33}	U^{12}	U^{13}	U^{23}
Na1	0.0124 (8)	0.0186 (8)	0.0328 (9)	0.0074 (6)	−0.0027 (7)	0.0034 (7)
Na2	0.0224 (8)	0.0224 (8)	0.0204 (12)	0.0112 (4)	0.000	0.000
Na3	0.0126 (10)	0.0170 (11)	0.0194 (11)	0.0103 (8)	0.000	0.000
Na4	0.0148 (7)	0.0148 (7)	0.0129 (11)	0.0074 (4)	0.000	0.000
Sr1	0.01062 (16)	0.01062 (16)	0.0063 (2)	0.00531 (8)	0.000	0.000
Ta1	0.00532 (9)	0.00532 (9)	0.00422 (11)	0.00266 (4)	0.000	0.000
P1	0.0065 (4)	0.0071 (4)	0.0078 (4)	0.0024 (3)	0.0007 (3)	0.0016 (3)
P2	0.0049 (6)	0.0057 (6)	0.0059 (5)	0.0027 (5)	0.000	0.000
O1	0.0198 (15)	0.0201 (15)	0.0130 (13)	0.0056 (13)	−0.0006 (10)	−0.0055 (10)
O2	0.0125 (13)	0.0169 (15)	0.0237 (13)	0.0098 (12)	0.0042 (11)	−0.0007 (11)
O3	0.0155 (13)	0.0197 (15)	0.0203 (14)	0.0071 (12)	0.0018 (12)	0.0146 (12)
O4	0.0068 (12)	0.0099 (12)	0.0132 (13)	0.0013 (10)	−0.0002 (9)	0.0039 (9)
O5	0.0166 (14)	0.0225 (15)	0.0152 (13)	0.0094 (12)	−0.0097 (11)	−0.0008 (10)
O6	0.0147 (19)	0.0119 (18)	0.0152 (18)	0.0075 (16)	0.000	0.000
O7	0.0044 (17)	0.0058 (16)	0.0120 (17)	0.0007 (13)	0.000	0.000

Table S3 Selected bond distances (Å) and angles (º) of $Na_{13}Sr_2Ta_2(PO_4)_9$.

Na1—O2^{i}	2.286 (3)	Sr1—O7^{xi}	2.642 (2)
Na1—O3^{ii}	2.422 (3)	Sr1—O7	2.642 (2)
Na1—O3^{iii}	2.478 (3)	Sr1—O7^{v}	2.642 (2)
Na1—O3	2.481 (3)	Sr1—O2^{xi}	2.645 (2)
Na1—O4	2.486 (3)	Sr1—O2^{xii}	2.645 (2)
Na2—O6^{iv}	2.617 (3)	Sr1—O2	2.645 (2)
Na2—O6^{i}	2.617 (3)	Sr1—O1^{xi}	2.812 (3)
Na2—O6^{v}	2.617 (3)	Sr1—O1^{xii}	2.812 (3)
Na2—O1^{ii}	2.622 (3)	Sr1—O1	2.812 (3)
Na2—O1^{vi}	2.622 (3)	Ta1—O4^{xiii}	1.946 (2)
Na2—O1	2.622 (3)	Ta1—O4	1.946 (2)
Na3—O6^{i}	2.292 (4)	Ta1—O4^{i}	1.946 (2)
Na3—O1	2.353 (2)	Ta1—O5	1.956 (2)
Na3—O1^{vii}	2.353 (2)	Ta1—O5^{i}	1.956 (2)
Na3—O7^{v}	2.472 (4)	Ta1—O5^{xiii}	1.956 (2)
Na3—O7	2.495 (4)	P1—O1	1.509 (2)
Na3—O6^{v}	2.512 (4)	P1—O3	1.515 (2)
Na4—O3^{viii}	2.345 (3)	P1—O2	1.520 (2)
Na4—O3^{ix}	2.345 (3)	P1—O4	1.602 (3)
Na4—O3^{x}	2.345 (3)	P2—O6	1.493 (4)
Na4—O2^{xi}	2.363 (3)	P2—O7	1.511 (3)
Na4—O2	2.363 (3)	P2—O5^{vii}	1.559 (3)
Na4—O2^{xii}	2.363 (3)	P2—O5	1.559 (3)
O4^{xiii}—Ta1—O4	91.45 (10)	O5^{i}—Ta1—O5^{xiii}	90.07 (11)
O4^{xiii}—Ta1—O4^{i}	91.45 (10)	O1—P1—O3	113.02 (16)
O4—Ta1—O4^{i}	91.45 (10)	O1—P1—O2	110.11 (16)
O4^{xiii}—Ta1—O5	87.71 (10)	O3—P1—O2	112.91 (15)
O4—Ta1—O5	90.81 (10)	O1—P1—O4	110.31 (14)

O4^{i}—Ta1—O5	177.61 (10)	O3—P1—O4	103.70 (14)
O4^{xiii}—Ta1—O5^{i}	177.61 (10)	O2—P1—O4	106.39 (14)
O4—Ta1—O5^{i}	87.71 (10)	O6—P2—O7	114.44 (19)
O4^{i}—Ta1—O5^{i}	90.81 (10)	O6—P2—O5^{vii}	111.86 (12)
O5—Ta1—O5^{i}	90.07 (11)	O7—P2—O5^{vii}	107.26 (13)
O4^{xiii}—Ta1—O5^{xiii}	90.81 (10)	O6—P2—O5	111.86 (12)
O4—Ta1—O5^{xiii}	177.61 (10)	O7—P2—O5	107.26 (13)
O4^{i}—Ta1—O5^{xiii}	87.71 (10)	O5^{vii}—P2—O5	103.4 (2)
O5—Ta1—O5^{xiii}	90.07 (11)		

Symmetry codes: (i) −*y*, *x*−*y*, *z*; (ii) −*x*+*y*, −*x*+1, *z*; (iii) *x*−*y*, *x*, −*z*; (iv) *x*, *y*+1, *z*; (v) −*x*+*y*+1, −*x*+1, −*z*+1/2; (vi) −*y*+1, *x*−*y*+1, *z*; (vii) *x*, *y*, −*z*+1/2; (viii) *x*−*y*+1, *x*, −*z*; (ix) *y*, −*x*+*y*, −*z*; (x) −*x*+1, −*y*+1, −*z*; (xi) −*y*+1, *x*−*y*, *z*; (xii) −*x*+*y*+1, −*x*+1, *z*; (xiii) −*x*+*y*, −*x*, *z*.

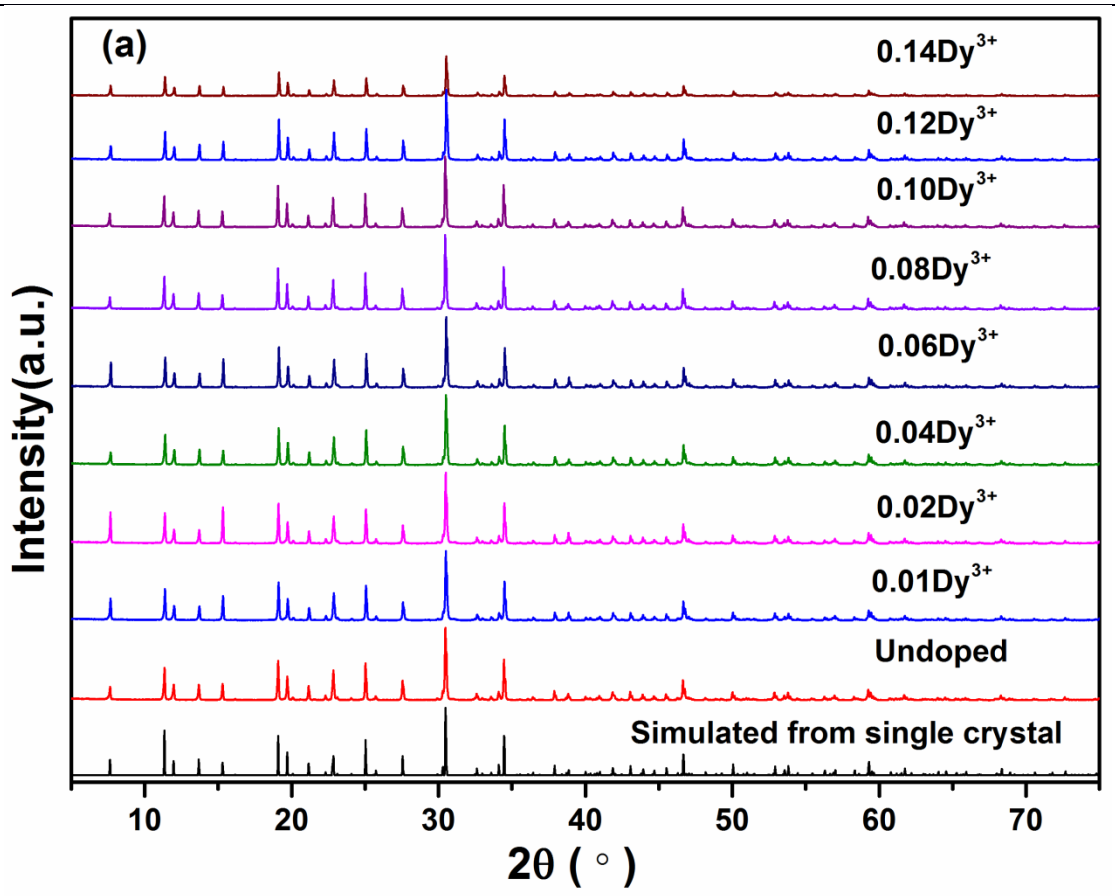

Figure S1 XRD patterns of powder samples $Na_{13}Sr_{2-x}Ta_2(PO_4)_9$:$xDy^{3+}$ (x=0, 0.01, 0.02, 0.04, 0.06, 0.08, 0.10, 0.12, 0.14) and simulated from single data.

References

Monkhorst, M. J. (1977). *Phys. Rev. B* **16**, 1748-1749.

Payne, M. C. (1992). *Rev. Mod. Phys.* 64, 1041-1045.

Perdew, J. P., Burke, K. & Ernzerhof, M. (1996). *Phys. Rev. Lett.* **77**, 3865-3868.

Petricek, V., Dusek, M. & Palatinus, L. (2014). *Z. Krist-New Cryst. S* **229**, 345-352.

Segall, M., Probert, M. & Hasnip, P. J. (2002). *J. Phys.: Condens. Matter* **14**, 2717-2744.

Spek, A. L. (2009). *Acta Crystallogr. Sect. D: Biol. Crystallogr.* **65**, 148-155.